Adopting Principles from Physics to Fatigue Crack Growth

Alderliesten, René

DOI
10.1201/9781003710493-9

Licence
Dutch Copyright Act (Article 25fa)

Publication date
2026

Document Version
Final published version

Published in
Fundamentals of Fatigue Fracture

Citation (APA)
Alderliesten, R. (2026). Adopting Principles from Physics to Fatigue Crack Growth. In *Fundamentals of Fatigue Fracture: Collective Works in the Memory of Prof. Mohan Ranganathan* (pp. 287-318). Jenny Stanford Publishing. https://doi.org/10.1201/9781003710493-9

Chapter Nine

Adopting principles from physics to fatigue crack growth

This chapter demonstrates how proper similitude utilizing principles from physics improves understanding of fatigue crack growth. After introducing elementary physical principles, a physical theory is outlined based on concepts separating available (driving) energy and material's intrinsic resistance. Several lessons learned are presented, after which these lessons are extrapolated to formulating the influence plasticity has on fatigue crack growth. It is illustrated how a proper energy balance, potentially can enable prediction of fatigue crack growth without typical Paris curves.

9.1 INTRODUCTION

Fatigue crack propagation is traditionally predicted with phenomeno-logical prediction models utilizing concepts based on stress, like the stress intensity factor (SIF) K [1]. After Paris [2-4], the crack growth rate da/dN is correlated in most cases to the SIF range ΔK using a scaling law, by many referred to as 'Paris law', despite that it is not a law proven from first principles but just a relationship. Although these relationships have demonstrated their engineering practicality and effectiveness in design as a predictive framework for fatigue crack growth, their incompleteness, and often non-compliance to fundamental laws from physics, has mostly been ignored in *scientific* literature. Instead, these scaling or power curves have served as fundamental basis in most research reported in *scientific* literature.

This lack of reflection against fundamental laws from physics has led to misinterpretations of observations, and incorrect explanations of several correction factors necessary in these phenomenological predictions [5].

Book Title
First Author & Second Author

www.jennystanford.com

Therefore, this chapter explains fatigue crack growth phenomena adopting principles from physics, shedding light on some discussions and disputes, explaining several phenomena previously reported, while illus-trating how future *science* could provide better predictive capabilities.

9.2 ELEMENTARY PRINCIPLES FROM PHYSICS

9.2.1 *Physical theory versus engineering prediction model*

Albeit predicting the fatigue crack growth rate with a power law like

$$\frac{da}{dN} = C\Delta K^m \tag{9.1}$$

yields successful predictions, dimensional analysis of eq. (9.1) reveals the formulation is flawed. Both *C* and *m* have units, while the exact unit for *C* depends on the value of *m*. This implies that both parameters must have a physical meaning, which is an aspect generally not elucidated upon in literature.

The graphical representation of Eq. (9.1) is often considered to illustrate the crack growth resistance of materials. Although not explicitly quantified, the resistance is then subject to the position of data or steepness of the curve in the graph. This is, however, a rather implicit form of characterizing the resistance, which for engineering predictions may suffice, but it does not allow an explicit correlation to the physical characterization of microstructural mechanisms.

9.2.2 *Strain energy perspective to cyclic loading*

When cyclically loading a structure between minimum and maximum load or stress, strain energy (work) is applied in a cyclic fashion, see Fig. 7.1 (a). The magnitude of this cyclic work depends not only on the load or stress range, but also on the mean level of the load cycle. Hence, while maintaining the same stress range, and thus the same *ΔK*, different mean stress levels yield the application of different amount of cyclic work. Inevitably, this difference in strain energy applied defines the amount of energy available for crack growth, and therefore the amount of *da/dN*.

Similarly, the increment of crack growth imposes a change in structural compliance, related to dissipation of elastic energy [6]. However, for tension-tension fatigue loading this energy dissipation is defined by the maximum load *only*, and not by the minimum load, see Fig. 9.1 (b).

Although the hysteresis between P_{min} and P_{max} is often considered for strain energy dissipation, the reduction in monotonic strain energy does illustrate that also energy dissipates below P_{min}.

Hence, where the 'driving force' in literature correlated to loading range P_{max}-P_{min}, is associated to cyclic work, the resistance to crack growth in this case is only characterized by the maximum load. Lumping both into a single parameter

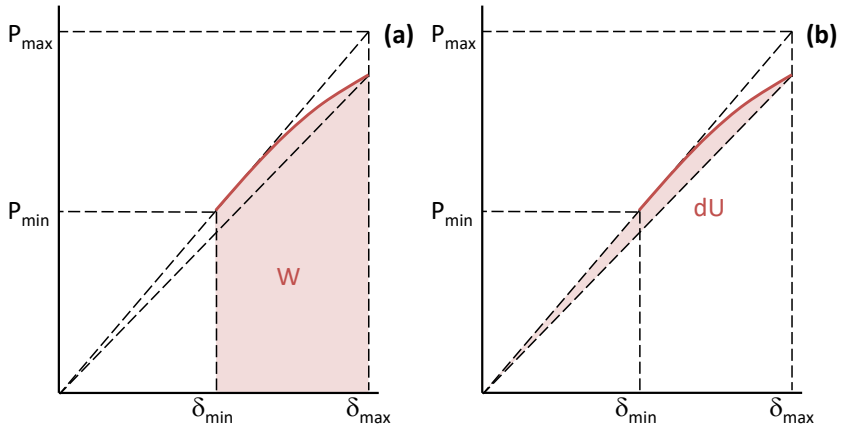

Figure 9.1. Illustration of how cyclic work W relates to $\Delta P=P_{max}-P_{min}$ (a), while the dissipated energy dU relates to P_{max} for cyclic tension-tension loading (b).

ΔK, therefore reduces the resolution in capturing all phenomena related to fatigue crack growth. Instead, 'resistance' should be separated from the 'driving force', for example through characterizing the phenomena with using at least two parameters; one to represent the applied work, and the other to represent the material's resistance to crack growth.

9.2.3 *Crack length versus fracture surface area*

Expressing crack growth in a change of crack length a, seems logical when describing through-thickness cracks in plates with constant thickness, but when describing cracks developing into a structure, this choice loses its similitude in physics.

For example, when the crack growth rate da/dN of a crack in a plate is constant, then the growth in fracture surface area (dA/dN) is also constant. However, when a circular corner crack grows with a constant da/dN, then the growth in fracture surface is increasing with its size with $\pi a/2$, see table 9.1.

Van Kuijk et al. [7] demonstrated that various corner crack to through-thickness crack transitions yield different and apparent irregular behaviour in Paris-graphs, typically attributed to small crack growth behaviour. However, with fracture surface area *A*, this irregular behaviour seems to be rather well explained.

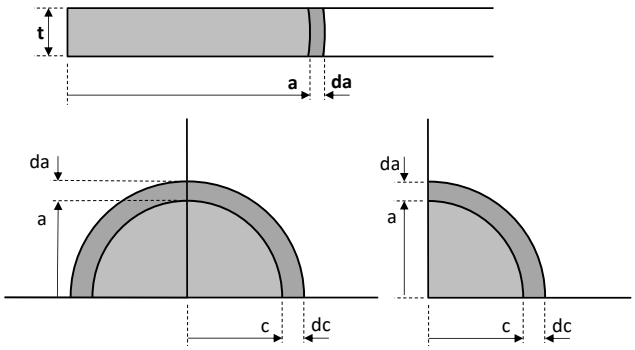

Figure 9.2. Comparison between a through-thickness crack propagating in a plate, and a surface or corner crack propagating into a solid.

Table 9.1. Relation between fracture growth rates *dA/dN* and fracture areas *A*

Type	Fracture area *A*	Growth rate *dA/dN*
Through-thickness crack	$A = a\,t$	$\frac{dA}{dN} = t\frac{da}{dN}$
Elliptical corner crack	$A = \frac{\pi}{4}\,a\,c$	$\frac{dA}{dN} = \frac{\pi}{4}(a\,dc + c\,da)$
Circular corner crack	$A = \frac{\pi}{4}\,a^2$	$\frac{dA}{dN} = \frac{\pi}{2}a\frac{da}{dN}$

9.3 FORCE AND RESISTANCE – AN ANALOGY FROM PHYSICS

To illustrate the theoretical concept of separating resistance from driving force, an analogy with sliding a box over the floor is proposed, see Fig. 9.3. When the force *F* is applied cyclically to the box, with value ranging between F_{min} and F_{max}, then the corresponding movement of the box relates to two parameters representing resistance: static friction F_{st} (stiction) that must be overcome before the box will move (analogy to fatigue threshold), and kinematic friction F_{kin} that defines how much 'driving force' is consumed while moving the box (intrinsic fatigue resistance).

For this problem, the equations of motion allow to translate the net force applied to the box, i.e. F-F_{st} upon start and F-F_{kin} while moving, through acceleration and velocity to displacement. With every load cycle range ΔF, the box will move with an increment Δx. Plotting the displacement rate dx/dN against the cyclic force ΔF, a curve will be obtained similar in shape to a Paris curve with a lower threshold (eg. Priddle [8]).
Corresponding to the parameter definition on the x-axis, that lower threshold is

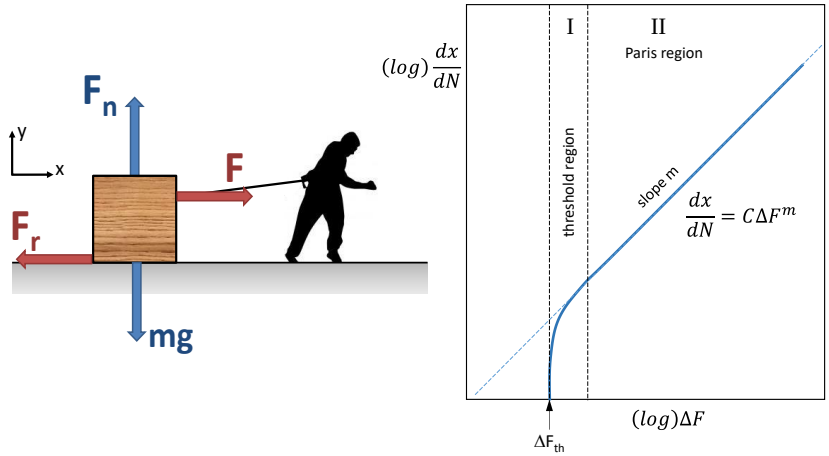

Figure 9.3. Analogy of a box (cyclically) pulled while sliding over the floor (left), and the 'resistance curve' following from the equations of motion (right).

defined as ΔF_{th} and it is in this case determined by static friction through F_{max}-F_{st}. The position and slope of the remainder of the curve are defined by the kinematic friction, see Fig. 9.3. The apparent dependence of threshold ΔF_{th} on the stress ratio $R=F_{min}/F_{max}$, is the artefact of plotting the effect of a constant F_{st} on a scale expressed as $\Delta F=F_{max}$-F_{st} (in the case of Fig. 9.3). Changing the mean value $F_{mean}=½(F_{max}+F_{min})$ relative to the constant value F_{st}, makes the threshold ΔF_{th} on the ΔF-scale move. This doesn't mean that the physical threshold is dependent of the stress ratio – because the static friction F_{st} is constant and independent of loading – but the R-dependency is in the ΔF (and ΔK) representation on the x-axis. It seems therefore more appropriate to define the lower threshold as K_{th} instead of ΔK_{th}, similar to the upper asymptote that is characterized by K_c instead of ΔK_c.

9.4 WHAT APPLIED CYCLIC WORK TELLS US ABOUT…

9.4.1 *…mean stress and stress ratio effects*

Many papers in literature discuss mean stress effects, for the case of fatigue life predictions, and stress ratio effects for fatigue crack growth [9]. The most interesting observation here is that most authors never consider that both effects essentially share the same cause: the mismatch between stress range (or amplitude) and cyclic work.
Hence, when comparing the general shapes of S-N curves with the typical 'Paris' curves, one can observe similarities in shape, see Fig. 9.4. The amplitude stress S_a is half the stress range ΔS, present in the expression for ΔK, while the life N is inversely proportional to da/dN.

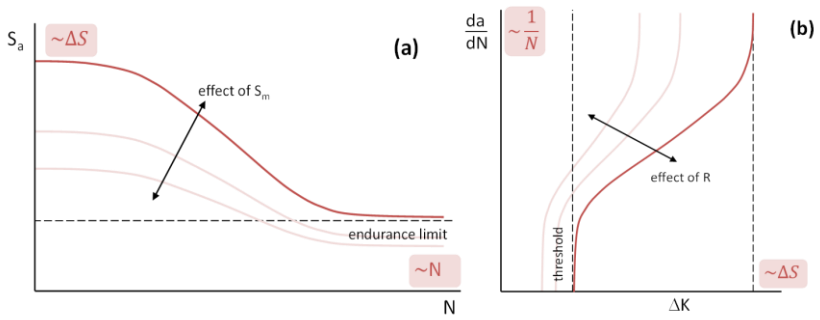

Figure 9.4. Similarity between mean stress effect and asymptotes in *S-N* curve (a)s and stress ratio effect and asymptotes in *da/dN-ΔK* plots (b).

The mean stress effect and stress ratio effect apparent in both graphs, are essentially introduced by taking the stress range ΔS or amplitude S_a in describing similitude. This can be illustrated easily considering the load-displacement curve for a linear elastic material in Fig. 9.5.

For a constant S_a or ΔS (ΔK), the increase in mean stress changes the work applied. More strain energy applied increases the crack growth rate *da/dN* and reduces the fatigue life *N*.

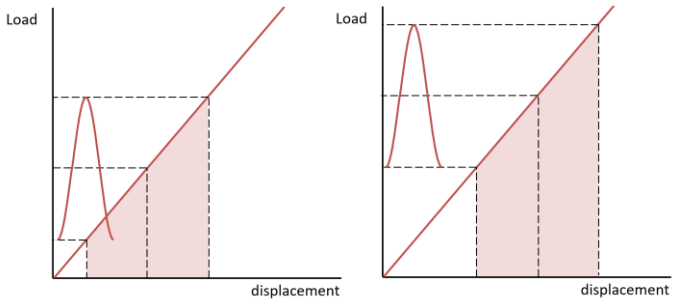

Figure 9.5. Influence of mean stress on the applied strain energy (work) for a fixed fatigue stress range applied to a linear elastic material.

9.4.2 *…Neuber's postulate and critical distances*

In the direct vicinity of a notch root, the peak stresses and strains can be approximated using Neuber's postulate [10], which can be expressed as

$$\sigma_{peak,pl}\varepsilon_{peak,pl} = \sigma_{peak,el}\varepsilon_{peak,el} = K_t^2 \frac{\sigma_{nom,el}^2}{E} \qquad (9.2)$$

where the subscript *peak,pl* refers to the elastic-plastic peak, while *peak,el* denotes the elastic peak, and *nom,el* refers to the elastic nominal stress in the net-section. Intuitively, the postulate sounds reasonable: the lower plastic peak stress multiplied with a higher plastic peak strain, could yield a similar product. Multiplying Eq. (9.2) with ½ however, yields a strain energy density expression, where ½σε describes the area under a linear elastic stress strain curve, see Fig. 1.6. Hence, in essence, Eq. (9.2) constitutes an strain energy balance, assuming that both shaded triangular areas in Fig. 1.6 have the same area.
Although this in concept sounds to have a basis in physics, it seems not entirely correct; to end up with the same amount of strain energy, the full area under the elastic-plastic stress-strain curve up to ($\sigma_{peak,pl}$,$\varepsilon_{peal,pl}$) should be equated to the area underneath the linear elastic curve up to ($\sigma_{peak,el}$,$\varepsilon_{peal,el}$).

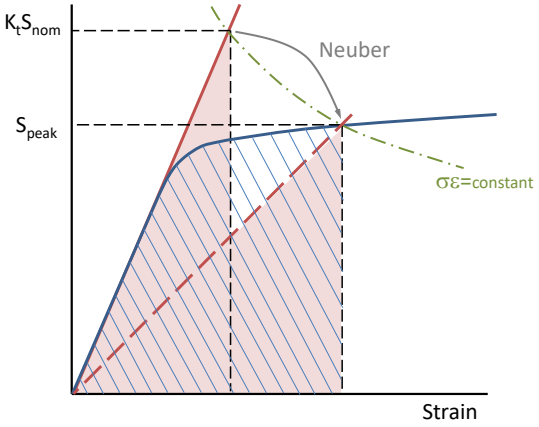

Figure 9.6. Illustration of the Neuber's postulate assuming the product of stress and strain

As illustrated in Fig. 9.6, this is not the case, which implies that there is no energy balance in the direct vicinity of the notch root. This obviously is explained through system boundaries in physics: moving from elastic to elastic-plastic, energy may redistribute to and from the area further way from the notch root. The formulation of Eq. (9.2) essentially takes the entire specimen's outer contours as system boundary, assuming that all energy within the specimen remains constant with the transition from elastic to elastic-plastic.

This is illustrated by that the local peak stresses and strains are expressed through a (gross) stress concentration factor and nominal (or gross) stresses away from the notch root. In essence, this is analogue to the concept of Alan Griffith for a cracked plate laying the foundation to fracture mechanics [6], where far field stresses are used.

Through Finite Element Analysis, one can demonstrate that the displacement of a notched plate under applied load changes, when moving from a pure elastic analysis to an elastic-plastic analysis. Fig. 9.7 illustrates this for a plate containing a central circular hole, comparing the applied work assuming linear elastic behaviour with the work applied assuming elastic-plastic response for either the same displacement or the same load.

Displacement controlled condition here refers to fixed grip conditions; redistribution of strain energy increases the specimen compliance a bit, but because that does not apply additional work to the specimen, this essentially releases strain energy. The force controlled condition, on the other hand, imposes the application of additional work with the increase in compliance through further displacement.

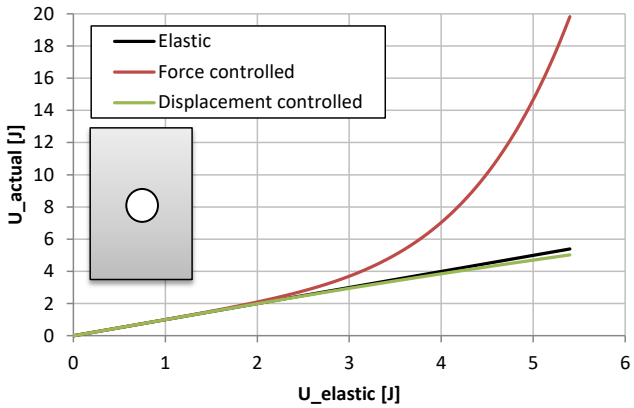

Figure 9.7. Illustration of the strain energy applied to a notch plate calculated through Finite Element Analysis assuming either load control or displacement control, compared to the linear elastic energy

What can be observed in Fig. 9.7 is that the error made with assuming strain energy balance is small for displacement controlled conditions, while for load controlled conditions the solutions clearly diverge with increasing load. This diverting curve for load controlled conditions, explains why Neuber's postulate generally is considered only valid with little plastic deformation, i.e. small scale yielding [11].

9.4.3 *…geometry corrections and finite width corrections*

In the expressions for the SIF, often correction factors are adopted to translate the infinite plate conditions for the exact solution to the finite dimensions of the problem at hand. Generally, this is referred to as geometry correction factors, i.e. they correct for a different geometry.
One typical geometry correction factor is the finite width correction *F(a)*, for which multiple solutions have been proposed in literature with the incentive to

increase accuracy in particular towards high values of crack over width (*2a/W)* [12-22]. Most of these studies developed a closed form solution for the finite width correction in relation to linear elastic stress field equations, like the ones developed in parallel by respectively Westergaard [17] and Koiter [18].
What seems to have received less attention is the underlying physics resulting in this need to correct. Essentially, this necessity emerges when methods based on stress do not entirely capture the physics of applying work or strain energy. Take for example the finite width correction *F(a)*. When a center-crack in a plate increases, the plate's compliance increases, measurable by a stiffness reduction. Loading with a constant load then implies that with increasing crack length an increased amount of work is applied, see Fig 9.8.
Studies addressing fatigue crack growth in monolithic metals and Fiber Metal Laminates (FMLs) demonstrated that the compliance change with crack length in

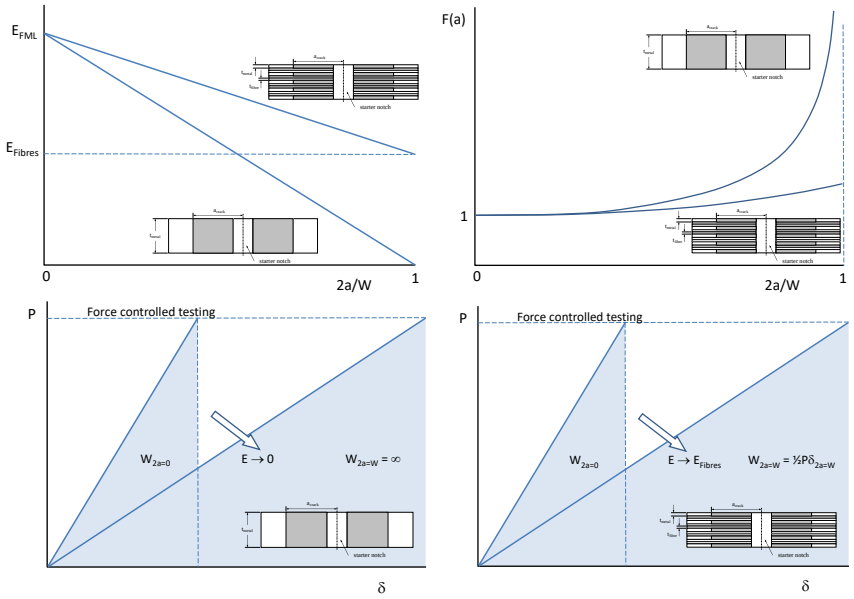

Figure 9.8. Stiffness reduction as function of crack length for monolithic metals and fiber-metal laminates (a) leads to different finite width corrections *F(a)* (b), which are explained by the corresponding ratios of work *($W_{2a}/W_{2a=0}$)* of both materials (c, d) [25].

both material systems is different, because in FMLs fibres bridging the crack maintain stiffness. This demanded different finite width corrections [23,24,25].
The implication of this observation is that the finite width correction in physics essentially constitutes a correction for applied work

$$\mathrm{F}(a) = \frac{W_a}{W_0} \tag{9.3}$$

where W_0 represents the work applied to an uncracked plate, and W_a the work applied to the plate with crack length a. This strain energy applied is not only dependent on geometry, but also on plate stiffness or compliance, which in turn it influenced by aspects like temperature [23]. Significant temperature variations in a fatigue test, therefore, may decrease the accuracy of finite width corrections proposed in literature!

Literature on fatigue life evaluation of composite materials often base their methodologies on stiffness reduction, which technically relates to the inverse of finite width corrections, i.e. the stiffness after N load cycles is $E_N = E_0/F(a)$.

$$E_N = \frac{E_0}{F(a)} \tag{9.4}$$

The amount of work after N load cycles therefore is described by

$$W_N = W_0 \frac{E_0}{E_N} \tag{9.5}$$

Even when constant amplitude *loading* is considered, one should acknowledge that degradation of stiffness, implies that the applied *work* is not constant, but continuously increasing!

9.4.4 *…crack closure corrections*

Despite that the stress ratio has an evident influence on the amount of work applied in a fatigue load cycle with a given stress range ΔS, as explained in section 9.4, many researchers have attributed the effect it has in the representation of crack growth resistance, illustrated in Fig. 9.4 b), to a phenomenon called crack closure.

This attribution can be explained by the hypothesis that ΔK describes similitude at the crack tip [26]. In such case, different crack growth rates da/dN for a given ΔK require further specification of this ΔK.

To explicitly account for the stress ratio, the SIF range ΔK was redefined to $\Delta K_{eff} = K_{max}-K_{op}$, where K_{op} is referred to as the opening (or closing) stress intensity factor. The hypothesis then is that only that part of the load cycle above the opening stress S_{op} contributes to crack growth. Following this definition, multiple crack closure corrections have been proposed [26-34], of which one is perceived better than the other depending on the data at hand.

However, assuming that the crack will only close at zero stress, through correlation of actual applied work to the phenomenological work defined by S_{max}-S_{op}, see Fig. 9.9, one can obtain a crack closure correction rather close to corrections proposed by Elber [27] and Schijve [28].

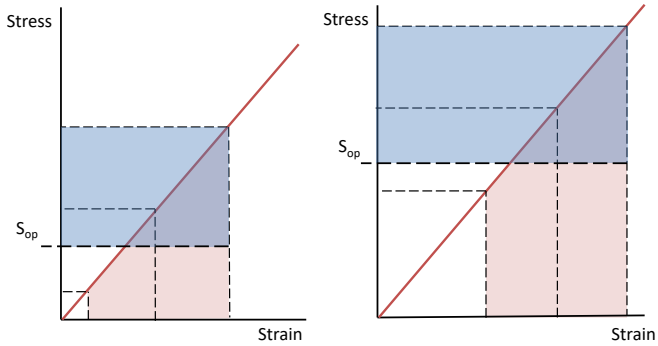

Figure 9.9. Illustration of how opening stress phenomenologically defines an amount of work equivalent to the actual work applied for a given stress ratio, while assuming crack opens at S = 0 MPa.

Presenting this observation at conferences [35] and in journals [5] received opposition, which perceived this presentation as an attempt to dispute crack closure as concept. However, as explained in a recent paper [36], crack closure as observation is not disputed. In fact, through elastic-plastic finite element simulations one can demonstrate plasticity induced crack closure occurs at stress levels greater than zero. These stress levels, however, do not coincide with the opening stress levels used in many crack closure corrections.
So how should we combine both observations? From the perspective of physics, the transition from a closed crack to an open crack, should be visible in a force-displacement curve through a transition in compliance, see Fig 9.10. A plate with a fully closed crack essentially has the stiffness equivalent to an uncracked plate, while a plate with open crack exhibits a greater compliance, increasing with crack length (section 9.4.3). This has been demonstrated experimentally [28] and numerically [36]. However, this stress S_{op} at which the crack tip physically opens, is different from the S_{op} in all crack closure corrections. Defining a phenomenological opening stress $S_{op,phen}$ such that an equivalent strain energy is obtained similar to the applied cyclic work, as illustrated in Fig. 9.10, provides opening stress levels corresponding to the crack closure corrections.

Van Kuijk et al. [36] demonstrated this through determining the physical opening stress $S_{op,phys}$ with finite element simulations at the moment the crack tip

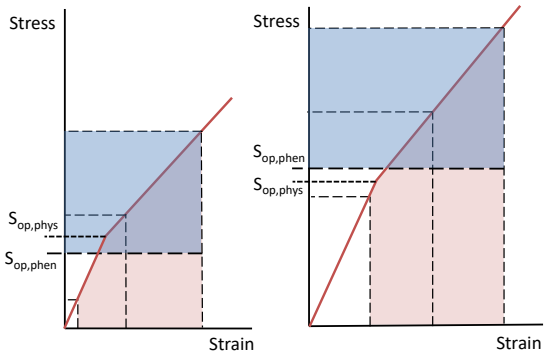

Figure 9.10. Illustration of how the phenomenological opening stress defines an amount of work equivalent to the actual work applied given a physical opening stress.

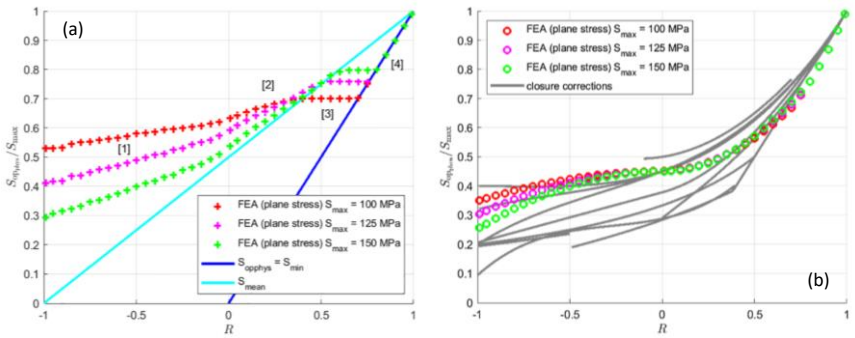

Figure 9.11. (a) Physical crack opening levels calculated through elastic-plastic finite element simulations and (b) corresponding phenomenological crack opening levels calculated through equating the applied work to an equivalent amount as illustrated in Fig 7.10 [36,37]

physically opens. Plotting this $S_{op,phys}$ against the stress ratio R, Fig. 9.11 (a), yields curves that do not agree with crack closure corrections. However, using this physical opening stress, to subsequently determine a phenomenological opening stress $S_{op,phen}$ such that the applied work corresponds to $(S_{max}\text{-}S_{op,phen})\varepsilon_{max}$, indeed yields the typical crack opening stress corrections, as illustrated in Fig. 9.11 (b). Hence, one should not assume that the opening stress level in all crack closure

corrections are the levels at which the crack tip physically opens, but realize that these levels essentially correct the stress-based method for the work applied, considering that as result of plasticity the crack tip opens at stress levels greater than zero.

9.5 THE INFLUENCE OF PLASTICITY IN CRACK GROWTH

9.5.1 *Relating crack growth to strain energy dissipation*

With the understanding from physics, that fatigue loading comprises the application of cyclic work with in conjunction with that applied work dissipation of energy through mechanisms like (for metals) plasticity and fracture surface formation, multiple scientists have attempted to correlate the energy dissipation to crack growth. Ranganathan et al. [38,39], for example, have tried to relate crack growth through experimental studies to the dissipation quantified through integrating the load-displacement curves. This relation appeared non-linear. Others have tried these relations in numerical studies, proposing to relate the crack growth linearly to the plastic energy dissipation [40], or to the reversed plastic zone ahead of the crack tip [41,42]. The difference between the latter two is, while both consider the dissipation per crack growth *dW/da* a material property, Cojocaru and Karlsson [42] did not assume it to be equal to the critical strain energy release rate.
Although all others consider that the plastic energy dissipation and energy release are involved in the fatigue crack growth process, it remains unclear which energy quantity exactly relates to crack growth and its formation of fracture surfaces [43]. To reveal which energy dissipation can be related quantitatively to crack growth, Quan at al. [43] proposed the energy conservation equation for static crack growth

$$\dot{W} = \dot{U}_a + \dot{U}_p + \dot{U}_e \tag{9.6}$$

where $\dot{W}$ is the external work differential (energy input), $\dot{U}_a$ the surface energy differential, $\dot{U}_p$ the plastic dissipation differential and U_e the differential of elastic strain energy stored. Similarly, Eq. (9.6), once integrated over the full cycle, can be expressed as

$$\frac{dW}{dN} = \frac{dU_a}{dN} + \frac{dU_p}{dN} + \frac{dU_e}{dN} \tag{9.7}$$

where *dW/dN* constitutes the external work done to the specimen over the entire cycle, described by the hysteresis in the force-displacement diagram.
In a combined experimental-numerical study, Quan et al. [43] quantified the components in Eq. (9.7). The combination with the detailed finite element analysis of the experiment, enabled the determination of the small energy

dissipation quantities through a global-local approach, where the local boundary deformations were taken from the experiment through digital image correlation.
The observation is that correlating the crack growth *da/dN* to either dU_p/dN or to dU_e/dN yields a non-linear trend that is subjective to apparent stress ratio effects. Only the energy dissipation component dU_a/dN is straightforwardly correlated to crack growth *da/dN*, which intuitively can be understood, because the surface energy per fracture surface area formed is assumed constant.
In a more detailed study, Van Kuijk [44] illustrated the concerns raised in the conclusions by Quan et al. [43]; the crack length relates to a projected crack surface, see section 9.2.3, while the true fracture surface through roughness and shear lips does not uniquely relate to the projected surface, see Fig. 9.12. Van Kuijk, assumed for the developing shear lips under 45° an increase relative to the projected area of factor $\sqrt{2}$, while for roughness he proposed to use a scale factor that could be related to various definitions of roughness.

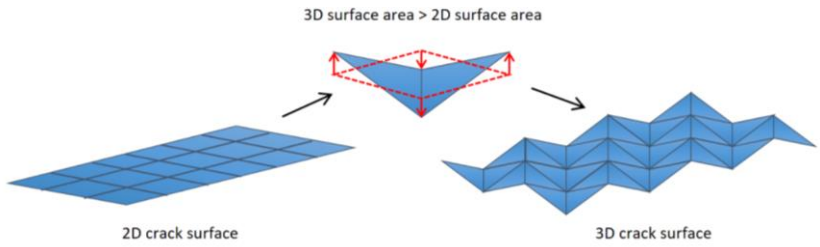

Figure 9.12. Illustration of how roughness increases the true fracture surface compared to projected crack area (or crack length) [44]

Similar to the latter proposal, Hogeveen [45], when fatigue testing aluminium fatigue crack growth in ambient laboratory air or in near vacuum conditions, could relate his observations through normalizing the fracture surface formation through surface roughness measured along the crack growth direction.
Hence, instead of crack length *a*, one should acknowledge that fracture surface *A* is created, where development of shear lips and roughness along the crack direction, changes the true fracture area relative to the projected area.

9.5.2 *Measuring plasticity contribution with potential drop through-the-cycle*

Generally, the potential drop technique is adopted to ease crack length measurements following recommendations from the ASTM standard [46]. Here,

Van Kuijk et al. [11] improved the resolution of the technique to the extent that measurements through the fatigue load cycle could be related to the contribution of the plastic zone ahead of the crack tip. The underlying hypothesis of the study was that the change in electric potential is not linearly related with the instantaneous crack increment *da*. The path of electric current is locally related to the actual crack increment, and through the plastic zone, also to the level of plastic deformation ahead of the crack tip. Both are influenced by the Poisson's effect, while crack tip plasticity is mostly affected by piezoresistivity [47].

The potential measurements in μV, despite amplifying, are extremely sensitive, which demonstrated the technique to be best applicable to intermediate to large crack lengths rather than small crack lengths. Even for these crack lengths, the signals experience scatter, which Van Kuijk et al. [48] solved by implementing a moving average technique within the measurement set-up. Van Kuijk justified this scatter reduction technique with the assumptions that cracks can only monotonically increase in length.

A typical observation is illustrated in Fig. 9.13. Initially the signal follows the sinusoidal shape of the load cycle applied, but once the crack tip developed the plastic zone, the electric potential exhibits a plateau. Taking the intersects between the plateau and the sinusoidal shape to determine the time for crack tip opening and closure, illustrate that the crack opening stress S_{op} is not identical to the

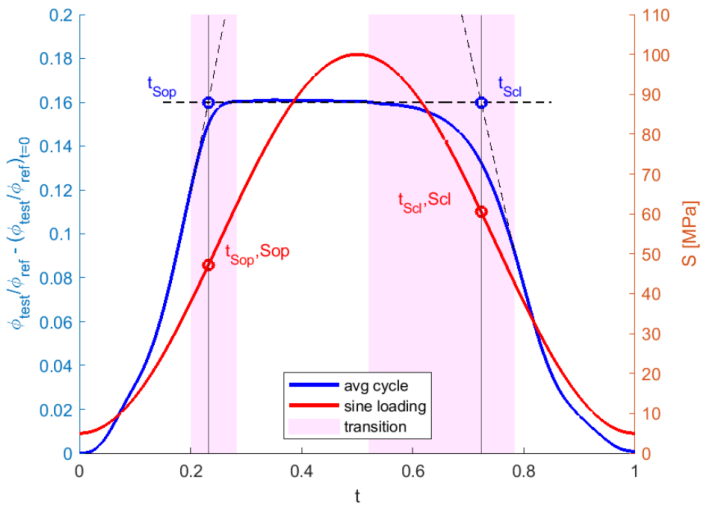

Figure 9.13. Illustration of electrical potential response relative to a sinusoidal load cycle; the potential plateau suggests balance between Poisson's effect and piezoresistivity. The magenta areas illustrate the crack opening and closure transition [48]

closure stress S_{cl}. While, this is occasionally acknowledged in literature, both stresses are often assumed to be the same in crack closure concepts [28]
Through correlating the results illustrated in Fig. 9.13 to digital image correlation performed on images taken with high speed camera, Van Kuijk observed that the peak strain within the plastic zone followed the plateau, while the location of that peak strain correlated to the sinusoidal load cycle. Based on these observat6ion, one can hypothesize that the plastic zone with particularly the peak strain within the zone shifts along the crack increment during a specific phase of the load cycle, i.e. above the physical crack tip opening level.

9.6 THEORETICAL APPROACH TO FATIGUE CRACK GROWTH

9.6.1 *Discrete and continuous strain energy balance in fatigue*

The energy balance expressed in Eq. (9.6) can be rewritten through integrating over a full load cycle to the form of Eq. (9.7). Here, one should note that the balance itself does not contain the number of cycles in the expression. This means that Eq. (9.6) is valid indifferent of the moment in a load cycle, or the number of load cycles applied. Hence, one may observe a discrepancy between theories from Physics, and prediction models used in Engineering: To predict the crack growth under given fatigue loading conditions, the engineer wants to express it against the number of load cycles. This number of load cycles, is however, not part of that theory, which in its formal formulation is continuous. To be able to predict, the theory must be discretized in order to incorporate the number if cycles N into the equations. However, through derivation, one never obtains an expression that explicitly contains N!

9.6.2 *Exploiting the analogy from physics*

To exploit the continuous energy balance from physics in an engineering prediction context with the number of cycles N, one could complement Eq. (9.6) with another physical analogy: the sliding box, see Fig. 9.3. The sliding box analogy is based on the equations of motion. The mass of the box multiplied with the gravitational acceleration g defines the normal force that the ground applies to the box. The friction force is expressed relative to that normal force through a friction coefficient. Essentially two coefficients are distinguished: with the box at rest, static friction defines the threshold force to be exceeded before the box

will move, while a moving box experiences kinematic or dynamic friction. The kinematic friction coefficient is generally somewhat lower than the static friction coefficient.
This analogy with fatigue crack growth helps in describing the fatigue crack growth, because similarly a threshold is present below which no crack growth is observed, illustrated with ΔF_{th} in Fig. 9.3, while growth of the crack depends on the crack growth resistance, i.e. the energy dissipated with the increment of the crack tip, illustrated by the position and slope of the curve in the so-called Paris region. This latter part is governed by the energy balance, Eq. (9.6) or in its discrete form Eq. (9.7), as illustrated hereafter.

9.6.3 *Predicting Paris crack growth resistance curves*

The work applied to a specimen can be expressed in terms of the strain energy density multiplied with the volume of the specimen, which for an uncracked plate is

$$\mathrm{W} = \frac{1}{2} S\varepsilon btL = \frac{S^2}{2E} btL \tag{9.8}$$

with S and ε the stress and strain, b, t and L respectively the plate width, thickness and length. When a crack is present, the plate will have more compliance; the longer the crack the more compliant the specimen is. Here, the observation that finite width correction factors essentially are energy corrections to stress based method, see section 9.4.3, can be exploited. Hence, the cyclic work applied can be represented by

$$\mathrm{W}_{max} - \mathrm{W}_{min} = \frac{S_{max}^2 - S_{min}^2}{2E} btL\sqrt{sec\left(\frac{\pi a}{W}\right)} \tag{9.9}$$

for the centre crack tension specimen geometry, where a is the half crack length.
The energy dissipation in one load cycle as result of crack growth in a plate with constant thickness, can be written as

$$\frac{dU_a}{dN} = \frac{dU_a}{dA}\frac{da}{dN} t\gamma\lambda \tag{9.10}$$

with $A=at$, and γ and λ factors for scaling with respectively roughness and with shear lip formation. For the shear lip planes under 45°, $\lambda=\sqrt{2}$, applied proportionally to the fraction of shear lips over fracture surface.
The free surface dU_a/dA represents the energy required to create the fracture surfaces, which for a bulk material may be considered constant. Typically, for aluminum 1 J/m^2 [49] can be assumed, which in Eq (9.10) becomes 2 J/m^2, because two (mating) crack surfaces are generated in crack growth.

With the major components dU_a/dA and t constant, Eq (9.10) illustrates why Quan et al. [43] observed an almost linear relationship between the crack growth da/dN and the energy dissipation dU_a/dN. Only the roughness and shear lips development, alter the linear dependency a bit.

The second component in Eq. (9.7), dU_p/dN, quantifies the strain energy dissipation through plasticity around the crack tip. The energy dissipation can be written as

$$\frac{dU_p}{dN} = \frac{dU_p}{dV_p}\frac{dV_p}{da}\frac{da}{dN} \tag{9.11}$$

where dU_p/dV_p represents the mean plastic energy density within the plastic zone, and dV_p/da the change in plastic volume V_p per crack increment da. The latter term, can be approximated adopting Irwin's plasticity model [50], assuming the plastic zone to be a cylinder with a height equal to the plate thickness t and a radius r_p

$$r_p = \frac{1}{\pi}\left(\frac{K}{S_{yield}}\right)^2 = \frac{1}{\pi}\left(\frac{S_{max}F(a)\sqrt{\pi a}}{S_{yield}}\right)^2 = aF^2(a)\left(\frac{S_{max}}{S_{yield}}\right)^2 \tag{9.12}$$

For the finite width correction $F(a)$, discussed in section 9.4.3, one can take the Feddersen's correction [13]

$$V_p = a^2 sec^2\left(\frac{\pi a}{W}\right)\left(\frac{S_{max}}{S_{yield}}\right)^4 \tag{9.13}$$

which gives after derivation

$$\frac{dV_p}{da} = 2\left(\frac{S_{max}}{S_{yield}}\right)^4 tsec^2\left(\frac{\pi a}{W}\right)\left[a + a^2\frac{\pi}{W}tan\left(\frac{\pi a}{W}\right)\right] \tag{9.14}$$

For the mean plastic energy density within the plastic zone dU_{pl}/dV_{pl} Van Kuijk

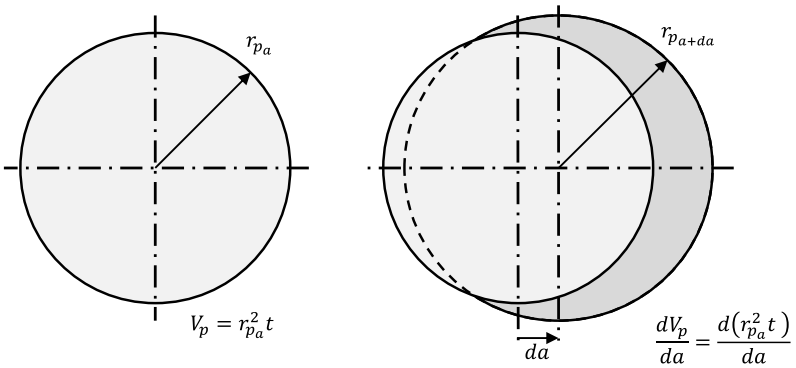

Figure 9.14. Illustration of the increase in cylindrical plastic volume according to Irwin through translation (crack increment) and radius r_p increase, after [44]

[44] proposed a generic description based on various studies

$$\frac{dU_p}{dV_p} = \pi\left(1 - 2\left(\frac{2a}{W}\right)^{\phi}\right)\left(\frac{S_{max}}{S_{yield}}\right)^2 \tag{9.15}$$

The last component in Eq. (9.7), i.e. dU_e/dN, represents the elastic energy stored due to the change in plastic volume. Essentially, the residual stress build up in the plate due to plasticity, relates to the elastic energy stored within the plate after unloading. Although with variable amplitude loading this plasticity induced elastic energy dissipation changes continuously, this can be ignored when developing Paris crack growth resistance curves, which are generally created with constant amplitude loading. For the case of constant amplitude loading, Van Kuijk assumed the elastic energy dissipation substantially smaller, but proportional to the plastic energy dissipation through

$$\frac{dU_e}{dN} \propto \frac{dU_p}{dN} \tag{9.16}$$

With this assumption, one can through a small constant scale factor, evaluate the strain energy dissipation through a load cycle, based on Eq. (9.6).
However, as discussed by Van Kuijk, this energy balance is continuous and therefore does not contain information about the number of cycles *N*. To evaluate crack growth using the energy balance, he proposes to utilize the moving box analogy from section 9.3, with assuming a sinusoidal load cycle with $F(t) \propto sin^2$, such that the maximum in the cycle, $F_{max} = U_{max}(a)$.

Van Kuijk [44] then considers two methods to calculate the input total work applied U_{max}, either directly through Eq. (9.8) or indirectly through the summation of the dissipation terms from Eqs. (9.10), (9.11), and (9.16).
In the moving box analogy, one has to define two constants for stiction and friction. For the stiction he proposes an arbitrary value of $0.9999U_{max}(a=0)$ to trigger crack growth in the first load cycle. Through Eq. (9.9) one can then expect crack growth to occur in all successive cycles. For the friction constant, he proposes to rely on the S_{op}/S_{max} relations from crack closure corrections. This instead could be calculated directly through using the methodology explained in section 9.4.4. However, while the approach in section 9.4.4 demonstrates that the corrections can be correct, equating the friction constant to the S_{op}/S_{max} relations, significantly reduces the computing time.
The *da/dN* value calculated through either of the two procedures can be integrated to crack length *a* versus number of cycles *N*, while the corresponding maximum stress S_{max} with the S_{op}/S_{max} relations is used to compute ΔK_{eff}. Plotting *da/dN* against ΔK_{eff} then yields the Paris crack growth resistance curves.

9.6.4 *Predicting fatigue crack growth through first principles*

The procedure in the previous section, therefore, can be used to predict crack growth curves, as demonstrated by Van Kuijk [44] and illustrated in Fig. 9.15, where the four tests in Table 9.2 are compared to a direct and indirect method. The direct method consist of the procedure using the sliding box analogy, in which the friction is calculated directly from the crack closure corrections. In the indirect method, an iterative scheme is adopted using the sliding box analogy to quantify the 'driving force', while the energy balance of Eq. (9.7) is used to describe the corresponding energy dissipation (resistance).

Table 9.2. Fatigue tests parameters of fatigue centre-crack tension tests

Test	Material	W [mm]	t [mm]	a_0 [mm]	S_{max} [MPa]	R	S_{yield} [MPa]	Ref
1	2024-T3	160	6.1	13.18	60	0	324	[44]
2	2024-T3	160	6.1	11.25	80	0.3	324	[44]
3	7075-T6	160	3.2	6.35	48.8	0.1	503	[43]
4	Fe520Nb	100	10	10	113	0.5	460	[51]

The stress intensity factors corresponding to the predicted crack growth can be calculated for each crack length, which enables composing the Paris crack growth resistance curves for the four tests, as illustrated in Fig. 9.16. Hence, through this

physics-based analogy one can predict fatigue crack growth essentially without having Paris crack growth curves a priori. In essence, only quasi-static stress-strain data is required to evaluate the strain energy dissipation in the plastic zone along with some generic assumptions on roughness and shear lip development.
Approximating the plastic dissipation through Irwin's plasticity relations is a rather rudimentary evaluation of the plastic energy contributions, as one may deduce from multiple numerical studies on this subject [38-43]. However, similar to these studies, the stress-strain relationship for the alloy considered can be used to capture in greater detail how much strain energy dissipates in the plastic zone, as replacement of Eqs. (9.14) and (9.15).

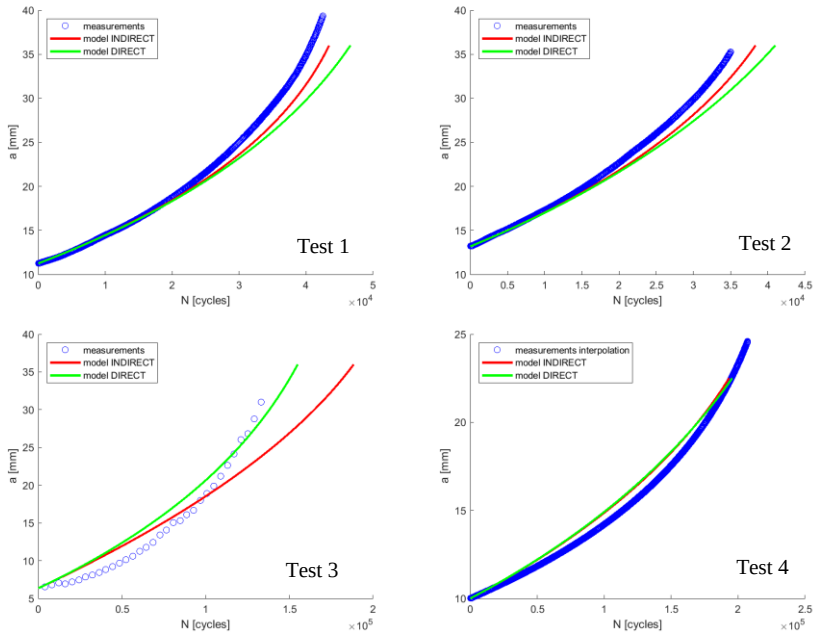

Figure 9.15. Crack growth curves predicted by Van Kuijk through both the direct and indirect method, in comparison with data from fatigue crack growth experiments, listed in Table 9.2 [44]

Where this concept requires further research, is the assumption on the elastic energy dissipation dU_e/dN. For constant amplitude loading the assumption on proportionality may be justified, for variable amplitude loading this certainly will not be true. Distinct load variations in the load spectrum will cause plasticity induced retardation or acceleration, which relate to the elastic energy stored in the structure due to plasticity effects. This is however, not the only aspect to be

addressed. As explained in section 9.4.4, the applied work varies depending on the physical crack opening, which is affected by the same plasticity effects. In other words, when predicting crack growth, one must separate the 'driving force' from 'resistance', where the interplay between both determine the crack growth, but plasticity affects both the applied work, and the strain energy dissipation.

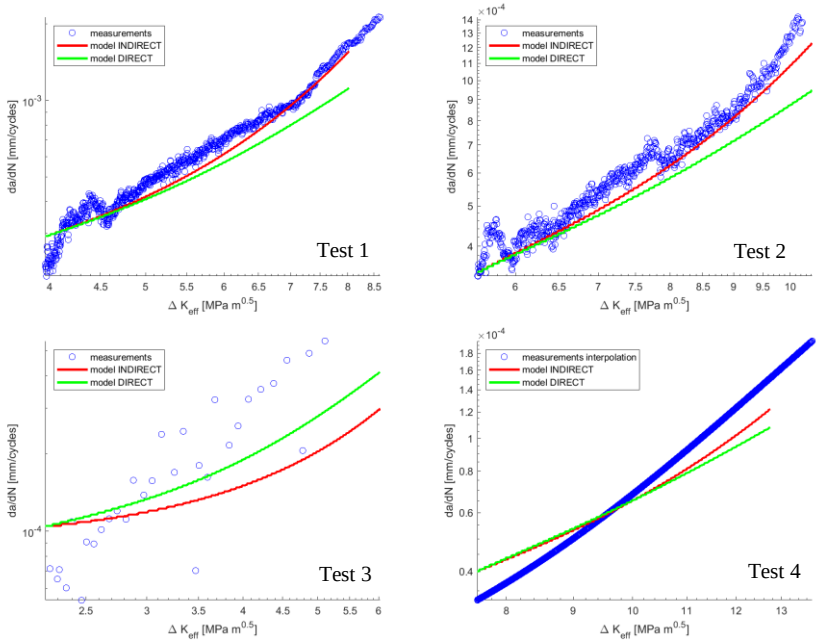

Figure 9.16. Paris resistance curves predicted by Van Kuijk through both the direct and indirect method, in comparison with data from fatigue crack growth experiments [44], listed in Table 9.2.

Hence, to develop this analogy to variable amplitude loading conditions, one must through Fig. 9.10 calculate the work applied including physical crack opening.
Then, the plastic energy dissipation term dU_p/dN must be evaluated, whereas for the plastic volume it can be evaluated whether the newly created plastic zones are formed within previous plastic volumes, or whether the plastic zone develops beyond prior plastic zones. Conceptually, this will be similar to the basis in current yield zone methods, like Willenborg [52] and Wheeler [53,54].
The plastic strain density in the plastic volume, i.e. dU_p/dV_p, requires further attention. Distinct load variations might affect the average strain energy density within the plastic zone, but this has not yet been demonstrated. Further evaluating

how plastic zone development under variable amplitude loading relates to applied work through plasticity induced crack opening, may in the end yield crack growth predictions without the necessity for Paris crack resistance curves, or prior art testing.

9.7 SUMMARY

Characterizing fatigue crack growth through the use of Paris-type relationships has been widely implemented in modern damage tolerance design tools. A vast amount of experimental data has been generated over many years that has been used to construct databases exploited in these tools. The practically of working with these methods, and the substantial effort put in generating the data ad developing the tools, will make this practice not go away.
The current chapter illustrates, however, how a more physics-based approach could have led to the same predictive capability without performing vast amounts of tests. It illustrates how current empirical curves can also be constructed through adopting strain energy approaches instead of stress based equations. While it likely will not change the practice of current engineering prediction, this does provide the underpinning to our understanding of fatigue crack growth in metallic materials and structures. It also allows to relate structural observations through their shape and sizes to mechanical properties of materials.

References

1. Irwin, G.R. (1957). Analysis of stresses and strains near the end of a crack traversing a plate, *ASME J Appl Mech*, **24**, pp. 361–364.
2. Paris, P., Gomez M., Anderson W. (1961). A rational analytic theory of fatigue. *Trend Eng*, **13**, pp. 9–14.
3. Paris, P. (1964). The fracture mechanics approach to fatigue, In: 10th Sagamore Army Materials Research Conference. Syracuse University Press, pp. 107–132.
4. Paris, P., Erdogan, F. (1963). A critical analysis of crack propagation laws, *J Basic Eng*, **85(4)**, pp. 528–33.
5. Alderliesten, R.C., (2016). How proper similitude can improve our understanding of crack closure and plasticity in fatigue, *Int. J. Fatigue*, **82**, pp. 263-273.
6. A.A. Griffith, The Phenomena of Rupture and Flow in Solids, Phil. Trans. Royal Soc London, Series A, 221 (1921), 163-198
7. Van Kuijk, J.J.A., Alderliesten, R.C., Benedictus, R. (2018). Fatigue crack surface area and crack front length: new ways to look at fatigue crack growth, *Proc. FATIGUE 2018*, MATEC Web of Conferences **165**, 13009.
8. E.K. Priddle. High cycle fatigue crack propagation under random and constant amplitude loadings. Int J Pressure Vessels & Piping, 1976, 4:77-92.

9. Pascoe, J.A., Alderliesten, R.C., Benedictus, R. (2017). On the physical interpretation of the R-ratio effect and the LEFM parameters used for fatigue crack growth in adhesive bonds, *Int. J. Fatigue*, **97**, pp. 162-176.
10. H. Neuber, Kerbspannungslehre, Theorie der Spannungskonzentration Genaue Berechnung der Festigkeit, Springer Berlin, Heidelberg, 2001
11. W.D. Pilkey, D.F. Pilkey, Peterson's Stress Concentration Factors. 3rd rev. John Wiley & Sons, 2008.
12. M. Isida. Crack tip stress intensity factors for the tension of an eccentrically cracked strip. Lehigh University, Department of Mechanics Report, 1965.
13. C. Feddersen. Discussion to: plane strain crack toughness testing. American Society of Testing and Materials, 1967: 410.
14. G.R. Irwin, H. Liebowitz, P. Paris. A mystery of fracture mechanics. Engineering Fracture Mechanics, 1968, 1: 235-236.
15. W.T. Koiter. Note on the stress intensity factors for sheet strips with cracks under tensile loads. Delft Technological University, Department of Mechanical Engineering.1965, Report No. 314.
16. J. R. Dixon. Stress distribution around a central crack in a plate loaded in tension: effect of finite width of plate. Journal of Royal Aeronautical Society, 1960, 64: 141-145.
17. H. M. Westergaard. Bearing pressures through a slightly waved surface or through a nearly flat part of a cylinder, and related problems of cracks. Journal of Applied Mechanics 1939, 61: 49-53.
18. W. T. Koiter. An infinite row of collinear cracks in an infinite elastic sheet. Ingenieur-Archiv, 1959, 28(1): 168-172.
19. O. L. Bowie, D. M. Neal. A note on the central crack in a uniformly stress strip. Engineering Fracture Mechanics, 1970, 2: 181-182.
20. D. P. Rooke. Width corrections in fracture mechanics. Engineering Fracture Mechanics, 1970, 1: 727-728.
21. H. Tada. A note on the finite width corrections to the stress intensity factor. Engineering Fracture Mechanics, 1971, 3: 345-347.
22. K.S. Ravi Chandran. Insight on physical meaning of finite-width-correction factors in stress intensity factor (K) solutions of fracture mechanics. Engineering Fracture Mechanics, 2017, 186: 399–409.
23. Zhao, Y., Alderliesten, R., Zhou, Z., Fang, G., Zhang, J., Benedictus, R. (2018). On the physics of applying finite width and geometry correction factors in fatigue crack growth predictions of GLARE, *Int. J. Fatigue*, **117**, pp. 189-195.
24. Zhao, Y., Alderliesten, R., Wu, Z., Zhou, Z., Fang, G., Zhang, J., Benedictus, R. (2019). Determining finite-width-correction factors for fatigue crack growth prediction in GLARE using the equivalent compliance method, *Int. J. Fatigue*, **127**, pp. 74-81.
25. R.C. Alderliesten, Fatigue and Fracture of Fibre Metal Laminates, Springer International Publishing 2017
26. J. Schijve, Fatigue of Structures and Materials, 2nd ed. (Springer Science+Business Media B.V., 2009).
27. W. Elber, The significance of fatigue crack closure, ASTM STP 486 (1971), 230–242.

28. J. Schijve, Fatigue crack closure, observations and technical significance, Tech. Rep. LR-485 (Delft University of Technology, Department of Aerospace Engineering, 1986).
29. A. U. De Koning, Crack growth prediction methods, Part 1: A survey, Tech. Rep. NLR TR 84121 L Part I (Nederlands Lucht- en Ruimtevaartcentrum, 1984).
30. J. C. Newman Jr., A crack opening stress equation for fatigue crack growth, Int. J. Fatigue 24, 131 (1984).
31. T. Iwasaki, A. Katoh, and M. Kawahara, Fatigue crack growth under random loading, International Journal of Naval Architecture and Ocean Engineering 20, 194 (1982).
32. M. Kurihara, A. Katoh, and M. Kawahara, Effects of stress ratio and step loading on fatigue crack propagation ratio, in Current research on fatigue cracks (Current Japanese Materials Research) (Elsevier Applied Science, London, 1987).
33. J. L. Overbeeke and J. de Back, The influence of stress relieving and R-ratio on the fatigue of welding joints, in Fatigue of welded constructions: international conference, Brighton, England, 7-9 April 1987, edited by S. Maddox (Welding Institute, United Kingdom, 1988) pp. 11–22.
34. J. A. F. O. Correia, A. M. P. De Jesus, P. M. G. P. Moreira, and P. J. S. Tavares, Crack closure effects on fatigue crack propagation rates: Application of a proposed theoretical model, Advances in Materials Science and Engineering 2016, 3026745 (2016).
35. R.C. Alderliesten (2015), How proper similitude principles could have improved our understanding about fatigue damage growth, A Siljander, K Vaaraniemi (Eds.) Proceedings of the 34th conference and the 28th symposium of the ICAF, 47-57.
36. Van Kuijk, J.J.A., Alderliesten, R.C., Benedictus, R. (2021). Unraveling the myth of closure corrections: Sharpening the definition of opening and closure stresses with an energy approach, *Int. J. Fatigue*, **143**, 106016.
37. Van Kuijk, J.J.A., Alderliesten, R.C., Benedictus, R. (2021). Erratum to "Unraveling the myth of closure corrections: Sharpening the definition of opening and closure stresses with an energy approach", *Int. J. Fatigue*, **143**, 106016.
38. Ranganathan N, Chalon F, Meo S. Some aspects of the energy based approach to fatigue crack propagation. Int J Fatigue 2008;30(10-11):1921–9.
39. Mazari M, Bouchouicha B, Zemri M, Benguediab M, Ranganathan N. Fatigue crack propagation analyses based on plastic energy approach. Comput Mater Sci 2008;41(3):344–9.
40. Smith KV. Application of the dissipated energy criterion to predict fatigue crack growth of Type 304 stainless steel following a tensile overload. Engng Fract Mech 2011;78(18):3183–95.
41. Klingbeil N. A total dissipated energy theory of fatigue crack growth in ductile solids. Int J Fatigue 2003;25(2):117–28.
42. Cojocaru D, Karlsson AM. Assessing plastically dissipated energy as a condition for fatigue crack growth. Int J Fatigue 2009;31(7):1154–62.
43. Quan, H., Alderliesten, R.C. (2021). The relation between fatigue crack growth rate and plastic energy dissipation in 7075-T6, *Eng.Fract.Mech*., **252**, 107765.
44. J.J.A. van Kuijk, Novel insights into the physics of fatigue crack growth, Theoretical and experimental research on the fundamentals of crack growth in isotropic materials, PhD dissertation, Delft University of Technology, 2022.
45. J. Hogeveen, Towards a proper understanding of fatigue crack growth and crack closure (M.Sc. thesis), (2016).

46. ASTM International, ASTM E647-15e1, standard test method for measurement of fatigue crack growth rates, ASTM International, West Conshohocken, PA (2015).
47. M. Morozov, G. Y. Tian, and P. J. Withers, Elastic and plastic strain effects on eddy current response of aluminium alloys, Nondestructive Testing and Evaluation 28, 300 (2013).
48. Van Kuijk, J.J.A., Alderliesten, R.C., Benedictus, R. (2021). Measuring crack growth and related opening and closing stresses using continuous potential drop recording, *Eng.Fract.Mech*., **252**, 107841.
49. A. J. Kinloch, Adhesion and Adhesives: Science and Technology (Springer Science & Business Media, London, 1987).
50. G.R. Irwin, Linear fracture mechanics, fracture transition, and fracture control, Eng. Fract Mech, 1, 1241 (1968)
51. Houdijk, P.A. (1993), The effect of specimen thickness and specimen geometry on the fatigue crack growth in Fe510Nb, MSc thesis, Faculty of Applied Sciences, Delft University of Technology (in Dutch).
52. Willenborg J., Engle, R.M., Wood, H.A., A crack growth retardation model using an effective stress concept, AFFDL-TR71-1, Air Force Flight Dynamic Laboratory, Wright-Patterson Air Force Base (1971)
53. Wheeler O. Spectrum loading and crack growth. J. Basic Engrg 94 (1972), 181-186
54. Finney M. Sensitivity of fatigue crack growth prediction (using Wheeler retardation) to data representation. J Test Eval 1989;17:74–8